12 pgs

M-Shell Electron Capture and Direct Ionization of Gold by 25-MeV Carbon and 32-MeV Oxygen Ions*

CONF-841117--47

DE85 006923

M.C. Andrews, F.D. McDaniel, J.L. Duggan
North Texas State University,+ Denton, Texas 76203

P.D. Miller, P.L. Pepmiller, H. Krause, T. Rosseel++
Oak Ridge National Laboratory,# Oak Ridge, Tennessee 37830

L.A. Rayburn
University of Texas, Arlington, Texas 76019

R. Mehta and G. Lapicki
East Carolina University, Greenville, North Carolina 27834

M-shell x-ray production cross sections have been measured for thin solid targets of Au for 25 MeV $^{12}_{6}C^{q+}$ (q=4,5,6) and for 32 MeV $^{16}_{8}O^{q+}$ (q=5,7,8). The microscopic cross sections were determined from measurements made with targets ranging in thickness from 0.5 to 100 $\mu g/cm^2$. For projectiles with one or two K-shell vacancies, the M-shell x-ray production cross sections are found to be enhanced over those by projectiles without a K-shell vacancy. The sum of direct ionization to the continuum (DI) and electron capture (EC) to the L, M, N... shells and EC to the K-shell of the projectile have been extracted from the data. The results are compared to the predictions of first Born theories i.e. PWBA for DI and OBK of Nikolaev for EC and the ECPSSR approach that accounts for energy loss, Coulomb deflection and relativistic effects in the perturbed stationary state theory.

*Travel to ORNL provided by Oak Ridge Associated Universities.

+Supported in part by the Robert A. Welch Foundation and the NTSU Organized Research Fund.

++Analytical Chemistry Division, Oak Ridge National Laboratory, Oak Ridge, Tn 37830

#Supported by DOE, Division of Basic Energy Sciences, contract No. DE-AC05-84OR21400 with Martin Marietta Energy Systems, Inc.

DISCLAIMER

Introduction

During a heavy ion-atom collision, the two primary mechanisms by which inner-shell vacancy production can occur are direct ionization (DI) by Coulomb ionization and electron capture (EC) by the projectile. There are several theories available to describe these processes. Direct ionization can be described within the framework of the plane wave Born approximation (PWBA)[1] in which the quantum mechanical initial and final state wave functions are approximated by plane waves.

The Oppenheimer-Brinkman-Kramer (OBK)[2] theory uses the Born approximation to describe the capture of a target electron by the projectile. This theory was modified by Nikolaev (OBKN)[3] to include non-relativistic screened hydrogenic wave functions and observed binding energies to calculate the electron capture cross sections.

A theory which describes DI is the perturbed stationary state formalism (PSS) developed by Brandt and Lapicki[4] that accounts for the perturbation of the target electrons by the ions.

This approach may include Coulomb deflection (C) of the projectile by the target, a target electron relativistic (R) description, and an accounting for projectile-energy loss (E) and is referred to as the ECPSSR.[5,6] This theory has also been developed for EC and extended by Lapicki[7] to M-shell ionization.

During the past few years, various experiments have been performed which allow tests of these theoretical approaches. A number of experiments with gas targets showed large effects of projectile charge state on inner-shell ionization.[8-11] The increases in target

inner-shell ionization for projectiles with K-vacancies over those without K-vacancies was attributed to electron transfer of a target electron to the projectile K-shell.[12]

For solid targets, the experiments were not as well understood because the electron configuration of the ion inside the target was not well known.[13] The effects of residual K-shell vacancies in the ion on solid target x-ray production have been reported by Hopkins[14] and Groeneveld et al.[15,16] They found that the target x-ray yield increased considerably when the ion beam first passed through the carbon backing of the target before passing through the target material and as the target thickness increased.

This target thickness/beam charge state effect was more directly approached by Gray et al.[17] and McDaniel et al.[18] when they measured K-shell x-ray yields as a function of target thickness for projectiles with zero, one, and two K-shell vacancies. Both groups found that the variation in target x-ray production with target thickness could be explained in terms of the number of K-vacancies in the projectile. As the projectile charge state increased, the amount of K-shell to K-shell EC from the target to the projectile increased.

McDaniel et al.[19] also measured L-shell x-ray yields as a function of the projectile charge state and target thickness. Results similar to those for the K shell were again explained by EC to vacancies in the projectile K shell.

More recently, Mehta et al.[20] have compared M-shell x-ray production due to direct ionization and electron capture in the first Born and perturbed stationary state formalisms and have found their experimental results to compare favorably with the ECPSSR.

In this work, we report on measurements of M-shell x-ray production cross sections for 2 MeV/amu $^{12}_{6}C^{q+}$ (q=4,5,6) and $^{16}_{8}O^{q+}$ (q=5,7,8) incident on various thicknesses of Au from 0.5 to 100 $\mu g/cm^2$. The measurements reported here are total cross sections from which (1) DI plus EC to the L, M,... shells and (2) EC to the K-shell can be inferred. They compare favorably to theoretical calculations of Brandt and Lapicki[4,7] for DI (Fig. 1) and Lapicki and McDaniel[6,7] for EC (Fig. 2).

Experimental Proceedure

The 6.5 MV EN Tandem Van de Graaff accelerator at the Oak Ridge National Laboratory was used to obtain ion beams of 25 MeV carbon and 32 MeV oxygen in several charge states. The beam was electromagnetically analyzed for energy and charge state. It then passed through a series of focusing lenses and collimators before impinging on the target.

The target was positioned as 45^{o} relative to the incident beam. An Ortec Si(Li) detector was placed at 90^{o} relative to the beam in such a manner so as to view the front or incident side of the target. The absolute efficiency of the Si(Li) detector was determined by calculating its theoretical efficiency at x-ray energies less than 10 keV and normalizing that to measurements of several calibrated radioactive sources as described in Ref. 21. This method yields efficiency results with an estimated uncertainty of approximately +-14%.

The Au targets used in this investigation were thin clean foils prepared by vacuum deposition of the target material onto carbon backings. These backings were monitored throughtout their preparation in order to insure that the targets were as contaminent free as possible. This procedure has been described in Ref. 22.

While x-rays were being measured by the Si(Li) detector, a solid state charged particle detector was simultaneously used to measure the Rutherford scattering of the incident particles. These results were used to determine the product of the number of charged particles incident upon the targets and the number of target atoms which were

then utilized to normalize the x-ray yields.[21]

The data analysis of the x-ray and Rutherford spectra was a two-fold process. After each spectrum was obtained, an initial analysis was made at ORNL by using a PDP 11/45 computer and a Hewlett Packard CRT with light pen capabilities. Each spectrum was plotted on the CRT and a background was drawn in by hand. The area above the background line was then fitted with a Gaussian distribution and an area was determined. Later a least squares fit of the entire spectrum was done using the fitting program FACELIFT[23] to improve on the initial data reduction. This algorithm uses a Gaussian distribution with a linear background as the fitting function. A typical spectra can be seen in Ref 24.

For all but the thinnest targets ($t < 1.5\ \mu g/cm^2$) the fits were in good agreement with the measured spectrum and have an estimated uncertainty of +-5% in the x-ray yields. Due to a significant build-up of silicon contamination, the uncertainty in the thinnest target yields were estimated to be +-35%. Thus the overall uncertainty (efficiency and yield) for $t > 1.5\ \mu g/cm^2$ is 8-17% while that for $t < 1.5\ \mu g/cm^2$ is approximately 40%.

Results

Figure 1 illustrates the M-shell x-ray production cross sections as a function of target thickness. The triangles represent cross sections $\sigma_{XM}^{(0)}$ for projectiles with no K-shell vacancies, and the squares and dots represent cross sections $\sigma_{XM}^{(1)}$ and $\sigma_{XM}^{(2)}$ for projectiles with one and two K-shell vacancies, respectively. The $\sigma_{XM}^{(0)}$ results are approximately constant within statistical uncertainties for all targets while the $\sigma_{XM}^{(1)}$ and $\sigma_{XM}^{(2)}$ results rise steadily as target thickness decreases.

The EC cross sections σ_{XM}^{EC} were determined by taking the difference between the one or two K-shell vacancy cross sections and the cross section due to DI plus EC to the L, M, N, ... shells predicted by the ECPSSR. The total x-ray production cross sections for incident projectiles with zero, one and two K-shell vacancies are listed in Table I. From these results, the EC cross sections σ_{XM}^{EC} for target M-shell capture to the projectile K-shell were calculated, where $\sigma_{XM}^{EC(M\rightarrow 1/2K)}$ and $\sigma_{XM}^{EC(M\rightarrow K)}$ are the electron capture cross sections for ions with one and two K vacancies, respectively. Figure 2 shows the EC cross sections as inferred by this method.

Theoretical ionization cross sections were converted to x-ray procuction cross sections by using fluorescence yields and Coster-Kronig rates from McGuire.[25] Along with the results obtained here, we have plotted data from Mehta *et al.*[20] for 35 MeV ^{19}F incident on Au.[9] As with the results obtained by Mehta *et al.* we find that while both the OBKN theory for EC and the ECPSSR overpredict σ_{XM}^{EC}, the latter is much closer to being in agreement.

In conclusion, we have measured the contribution to M-shell ionization by DI and EC and compared the results to predictions based on the first Born theory (OBKN) and the perturbed stationary states theory (ECPSSR) for EC. We have found the ECPSSR to be in much better agreement for both the one and two K-shell vacancy cases than the first Born results.

Acknowledgements

We would like to thank R.L. Watson and C. Fulton of Texas A&M University for providing us with the program FACELIFT used in the spectrum analysis. The North Texas State University work is supported in part by the Robert A. Welch Foundation and the NTSU Organized Research Fund. The Oak Ridge National Laboratory is supported by DOE, Division of Basic Energy Sciences, Contract No. DEAC0584OR21400 with Martin Marietta Energy Systems, Inc. Travel to ORNL provided in part by Oak Ridge Associated Universities.

References

1. D.E. Johnson, G. Basbas, and F.D. McDaniel, At. Data and Nucl. Data Tables 24 (1979) 1.
2. J.R. Oppenheimer, Phys. Rev. 31 (1928) 349; H.C. Brinkman and H.A. Kramers, Proc. Acad. Sco. (Amsterdam) 33 (1930) 973.
3. V.S. Nikolaev, Sh. Eskp. Theor. Fiz. 51 (1966) 1263 [Sov. Phys.-JETP 24, (1967) 847].
4. W. Brandt and G. Lapicki, Phys. Rev. A23 (1981) 1717, and references therein.
5. G. Lapicki and W. Losonsky, Phys. Rev. A15 (1977) 896.
6. G. Lapicki and F.D. McDaniel, Phys. Rev. A22 (1980) 1896; A23 (1981) 975.
7. G. Lapicki, Bull. Am. Phys. Soc. 26 (1981) 1310.
8. J.R. MacDonald, L.M. Winters, M.D. Brown, T. Chiao, and L.D. Ellsworth, Phys. Rev. Lett. 29 (1972) 1291; L.M. Winters, J.R. MacDonald, M.D. Brown, T. Chiao, L.D. Ellsworth, and E.W. Pettus, Phys. Rev. A8 (1973) 1835.
9. J.R. Mowat, I.A. Sellin, D.J. Pegg, R.S. Peterson, M.D. Brown, J.R. MacDonald, Phys. Rev. Lett. 30 (1973) 1289.
10. F. Hopkins, R. Brenn, A.R. Whittemore, N. Cue, V. Dutkiewicz, and R.P. Chaturvedi, Phys. Rev. A13 (1976) 74.
11. C.W. Woods, R.L. Kauffman, K.A. Jamison, N. Stolterfoht, and P. Richard, Phys. Rev. A13 (1976) 1358.
12. A.M. Halpern and J. Law, Phys. Rev. Lett. 31 (1973) 4.
13. H.D. Betz, Rev. Mod. Phys. 44 (1972) 405.
14. F. Hopkins, Phys. Rev. Lett. 35 (1975) 270.

15. K.O. Groeneveld, B. Kolb, J. Schader, and K.D. Sevier, Z. Physik A 277 (1976) 13.

16. K.O. Groeneveld, B. Kolb, J. Schader, and K.D. Sevier, Nucl. Instr. and Meth. 132 (1976) 497.

17. T.J. Gray, P. Richard, R.K. Gardner, K.A. Jamison, and J.M. Hall, Phys. Rev. A14 (1976) 1333; T.J. Gray, P. Richard, G. Gealy, and J. Newcomb, Phys. Rev. A19 (1979) 1424.

18. F.D. McDaniel, J.L. Duggan, G. Basbas, P.D. Miller, and G. Lapicki, Phys. Rev. A16 (1977) 1375.

19. F.D. McDaniel, A. Toten, R.S. Peterson, J.L. Duggan, S.R. Wilson, J.D. Gressett, P.D. Miller, and G. Lapicki, Phys. Rev. A19 (1979) 1517.

20. R. Mehta, J.L. Duggan, F.D. McDaniel, M.C. Andrews, G. Lapicki, P.D. Miller, L.A. Rayburn, and A.R. Zander, Phys. Rev. A28 (1983) 2722.

21. R. Mehta, J.L. Duggan, J.L. Price, F.D. McDaniel, and G. Lapicki, Phys. Rev. A26 (1983) 1883.

22. P.M. Kocur, J.L. Duggan, R. Mehta, J. Robbins, and F.D. McDaniel, IEEE Trans. Nucl. Sci. NS-30 (1983) 1580.

23. FACELIFT is a least squares routine which fits several gaussian peaks plus a linear background simultaneously. It was obtained from R. Watson at the Physics Department, Texas A&M University.

24. R. Mehta, J.L. Duggan, F.D. McDaniel, M.C. Andrews, R.M. Wheeler, R.P. Chaturvedi, P.D. Miller, G. Lapicki, IEEE Trans. Nucl. Sci. NS-28, No. 2, 1122 (1981).

25. E.J. McGuire, Phys. Rev. A5 (1972) 1043.

Table I.

M-shell x-ray production cross sections of Au. From top to bottom, the cross sections are for zero, one, and two K-shell vacancies in the projectile and the inferred EC cross sections for one and two K-shell vacancies. Cross section units are 10^{5}b. Uncertainties of 40% for these thinnest targets result principally from Si(Li) detector efficiency (+-14%) and x-ray yield determination (+-35%).

Cross Sections	Projectile	$_{6}C$	$_{8}O$	$_{9}F^{*}$
	E/M (MeV/AMU)	2.08	2.00	1.84
	Z_1/Z_2	0.076	0.101	0.114
	$v_1/v_{2M_{4,5}}$	0.473	0.464	0.445
$\sigma_{XM}^{(0)}$	First Born	0.68	1.18	3.12
	ECPSSR	0.58	0.94	1.23
	Exp.	0.65 +_ 0.19	1.38 +_ 0.41	1.35 +_ 0.33
$\sigma_{XM}^{(1)}$	First Born	1.48	4.88	17.5
	ECPSSR	0.82	2.78	2.85
	Exp.	0.80 +_ 0.12	1.68 +_ 0.25	2.32 +_ 0.33
$\sigma_{XM}^{(2)}$	First Born	2.07	7.68	31.6
	ECPSSR	0.99	2.77	4.46
	Exp.	0.82 +_ 0.12	1.83 +_ 0.27	4.56 +_ 0.70
$\sigma_{XM}^{EC(M\rightarrow1/2K)}$	First Born	0.80	3.70	14.1
	ECPSSR	0.24	1.05	1.61
	Exp.	0.22 +_ 0.10	0.74 +_ 0.20	0.97 +_ 0.40
$\sigma_{XM}^{EC(M\rightarrow K)}$	First Born	1.39	6.50	28.5
	ECPSSR	0.41	1.83	3.23
	Exp.	0.24 +_ 0.10	0.89 +_ 0.21	3.21 +_ 0.70

*FLUORINE DATA ARE FROM REFERENCE 20.

Figure 1.

M-shell x-ray production cross sections vs. target thickness. The dot-dash line represents the cross section for direct ionization plus electron capture to the L-, M-, ... shells in the ECPSSR formalism. The uncertainty of the data is +-17% for all but the thinnest target, which carries an uncertainty of +-40%.

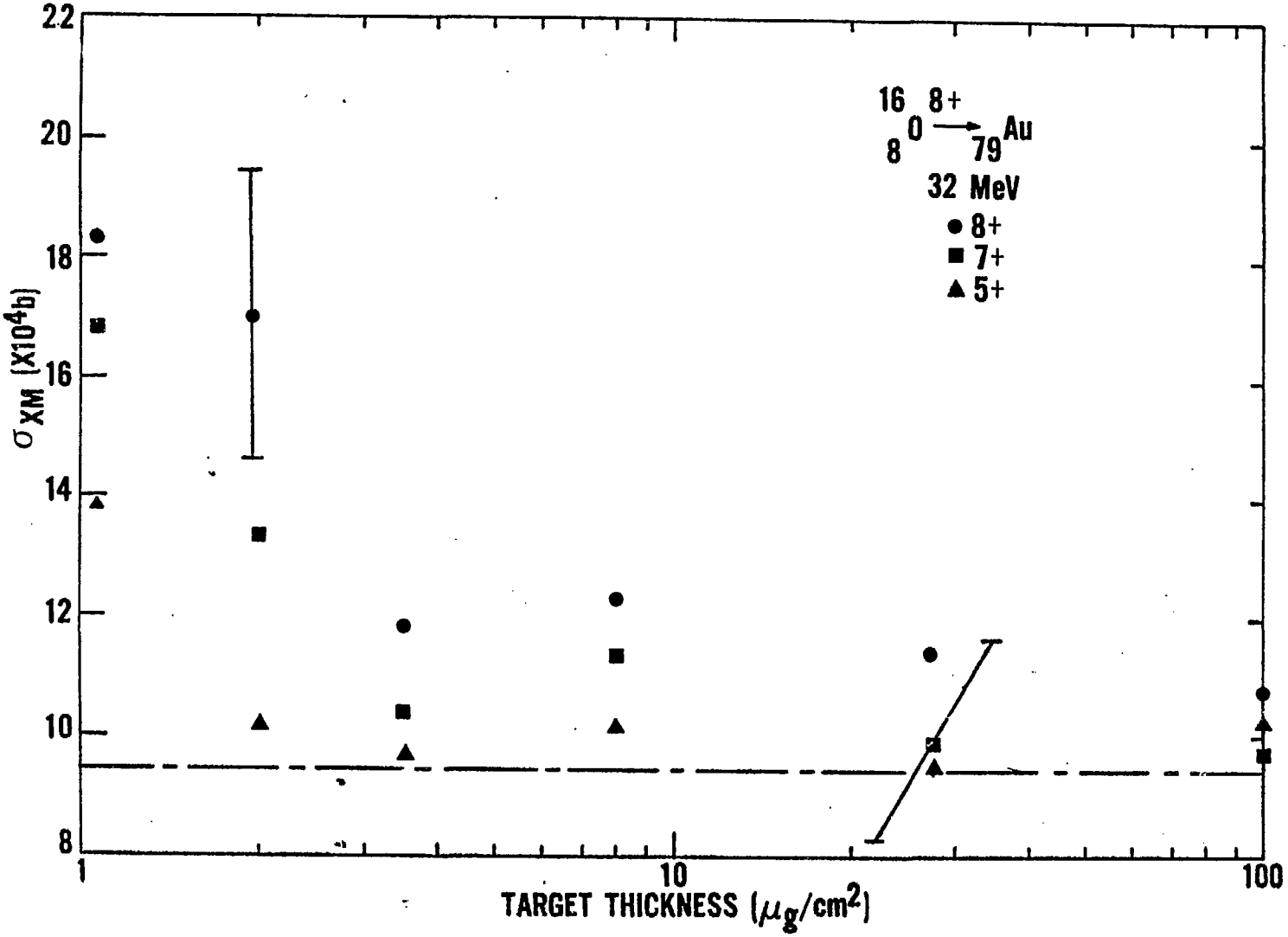
22
20
18
16
14
12
10
8
σ_{XM} (X10^{4}b)
1
10
100
TARGET THICKNESS (μ_g/cm^2)
$^{16}_{8}O^{8+} \rightarrow {}^{}_{79}Au$
32 MeV
8+
7+
5+

Fig. 1

Figure 2.

Inferred EC cross sections for projectiles of atomic number Z_1 with one ($q=Z_1-1$) K-shell vacancy and two ($q=Z_1$) K-shell vacancies verses Z_1/Z_2. The ion energies are 25, 32, and 35 MeV for carbon, oxygen, and fluorine, respectively. The fluorine data are from Reference 20.[5,6,7] The solid curves follow the ECPSSR calculations for EC, and the dashed curves are according to the first Born approximation[2,3]. These curves are drawn in an approximate manner between Z_1 =6,8, and 9 to the extent that all ions have nearly the same velocity (2 MeV/amu).

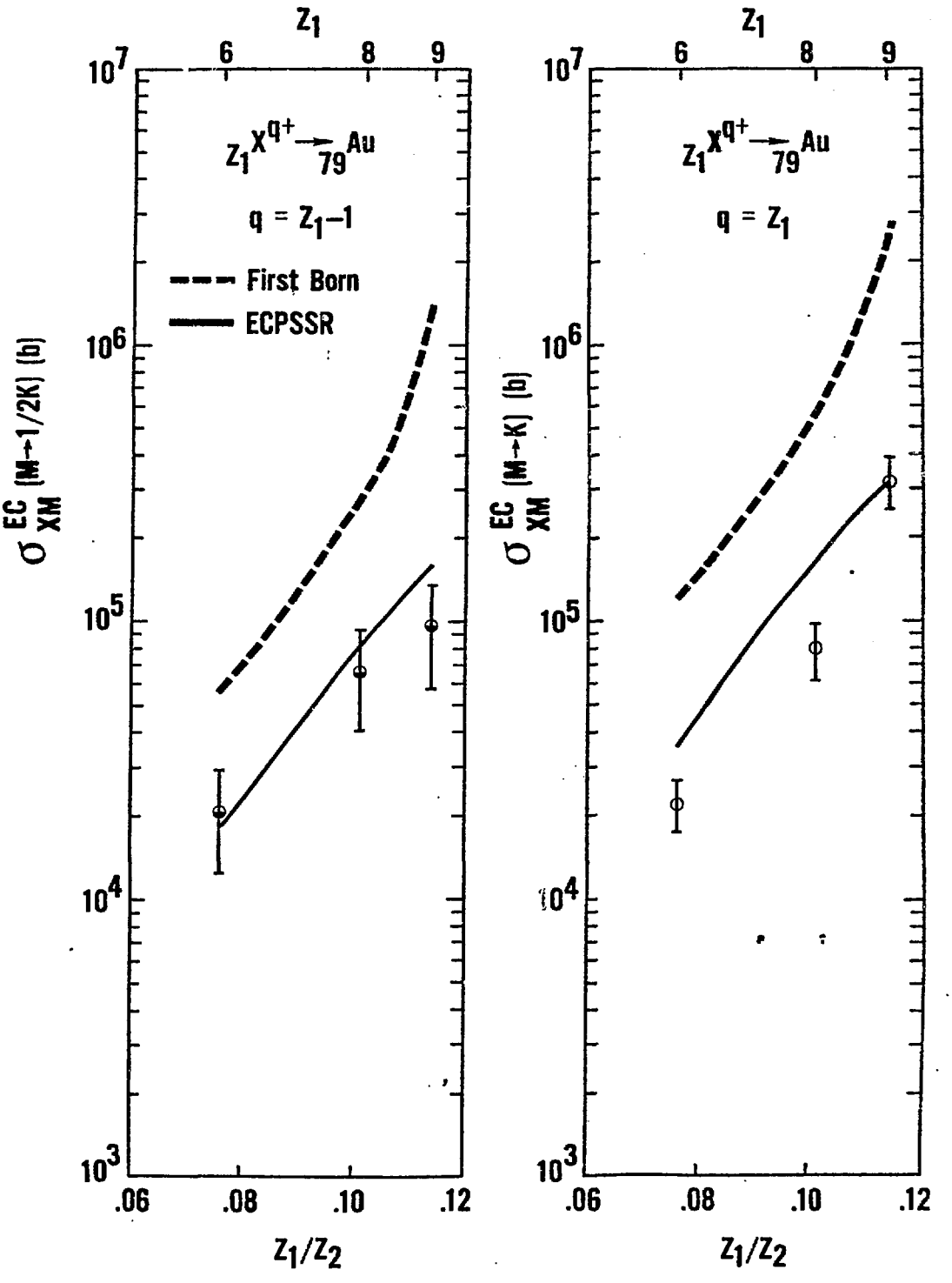
Z_1
6
8
9
10^7
10^6
10^5
10^4
10^3
$Z_1 X^{q+} \rightarrow {}_{79}Au$
$q = Z_1 - 1$
First Born
ECPSSR
σ_{XM}^{EC} (M→1/2K) (b)
.06
.08
.10
.12
Z_1/Z_2
Z_1
6
8
9
10^7
10^6
10^5
10^4
10^3
$Z_1 X^{q+} \rightarrow {}_{79}Au$
$q = Z_1$
σ_{XM}^{EC} (M→K) (b)
.06
.08
.10
.12
Z_1/Z_2